

CHEMISTRY OF MATERIALS

VOLUME 19, NUMBER 9

MAY 1, 2007

© Copyright 2007 by the American Chemical Society

Communications

Appearing, Disappearing, and Reappearing Fumed Silica Nanoparticles: Tapping-Mode AFM Evidence in a Condensation Cured Polydimethylsiloxane Hybrid Elastomer

Shinsuke Inagi,^{†,‡} Tomoki Ogoshi,^{†,‡} Junpei Miyake,^{†,‡} Massimo Bertolucci,[§] Tomoko Fujiwara,[†] Giancarlo Galli,[§] Emo Chiellini,[§] Yoshiki Chujo,[‡] and Kenneth J. Wynne^{*,†}

Chemical and Life Science Engineering Department,
School of Engineering, Virginia Commonwealth University,
601 West Main Street, Richmond, Virginia 23284-3028,
Department of Polymer Chemistry, Graduate School of
Engineering, Kyoto University, Katsura, Nishikyo-ku,
Kyoto 615-8510, Japan, and Dipartimento di Chimica e
Chimica Industriale, Università di Pisa, Udr Pisa-INSTM,
Via Risorgimento 35, 56126 Pisa, Italy

Received November 10, 2006

Revised Manuscript Received March 5, 2007

Hybrid nanocomposite materials have received considerable attention in recent years, opening a wide range of opportunities for new materials.^{1–10} One nanocomposite subset includes soft hybrids based on poly(dimethylsiloxane)

(PDMS).^{11–14} PDMS hybrids are hydrophobic, have low-temperature elasticity ($T_g = -123\text{ }^\circ\text{C}$), and display good hemocompatibility and biocompatibility.¹⁵ We have focused on PDMS hybrid surface science, including dihydroxy-terminated PDMS ($\text{HO}(\text{Me}_2\text{SiO})_n\text{H}$) cross-linked by condensation with fluorinated alkoxy-silanes¹⁶ or poly(diethoxysiloxane) (PDES).¹⁷ These studies and those on Pt-cured divinyl PDMS revealed time-dependent surface morphologies and the intrinsic wetting behavior of PDMS coatings.¹⁸

Hydrosilylation and condensation-cured PDMS networks are weak materials usually needing fillers for good mechanical properties.^{19–21} The customary filler for many applications, including biomedical elastomers,¹⁵ is amorphous fumed silica nanoparticles (FSN), which consist of nanoparticles and clusters. FSN may be untreated (U-FSN) or trimethylsilylated (T-FSN). Trimethylsilylated fumed silica is extensively used in commercial processes not only to improve

* Corresponding author. E-mail: kjwynne@vcu.edu.

[†] Virginia Commonwealth University.

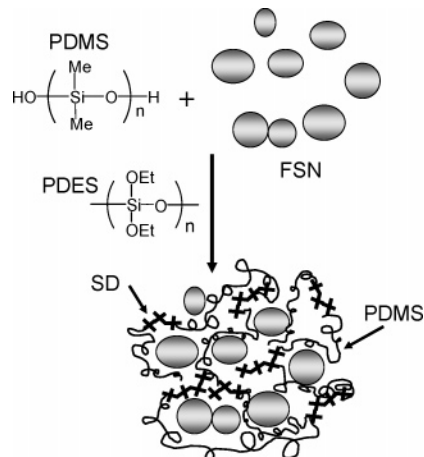
[‡] Kyoto University.

[§] Università di Pisa.

- (1) Wen, J.; Wilkes, G. L. *Chem. Mater.* **1996**, *8*, 1667.
- (2) Novak, B. M. *Adv. Mater.* **1993**, *5*, 422.
- (3) Giannelis, E. P. *Adv. Mater.* **1996**, *8*, 29.
- (4) Chujo, Y.; Tamaki, R. *MRS Bull.* **2001**, *26*, 389.
- (5) B. Boury, R. J. P. Corriu, *Chem. Commun.* **2002**, 795.
- (6) Corriu, R. J. P.; Lalexerq, D. *Angew. Chem., Int. Ed.* **1996**, *35*, 1420.
- (7) Special issue for organic-inorganic nanocomposite materials. *Chem. Mater.* **2001**, *13*.
- (8) Ogoshi, T.; Itoh, H.; Kim, K.-M.; Chujo, Y. *Macromolecules* **2002**, *35*, 334.
- (9) Ogoshi, T.; Chujo, Y. *Macromolecules* **2003**, *36*, 654.
- (10) Ogoshi, T.; Chujo, Y. *Macromolecules* **2005**, *38*, 9110.

- (11) Zhang, Z.; Sherlock, D.; West, R.; West, R.; Amine, K.; Lyons, L. J. *Macromolecules* **2003**, *36*, 9176.
- (12) Sur, G.-S.; Mark, J. E. *Eur. Polym. J.* **1985**, *21*, 1051.
- (13) Huang, H. H.; Orler, B.; Wilkes, G. L. *Macromolecules* **1987**, *20*, 1322.
- (14) Julián, B.; Gervais, C.; Rager, M.-N.; Maquet, J.; Cordoncillo, E.; Escribano, P.; Babonneau, F.; Sanchez, C. *Chem. Mater.* **2004**, *16*, 521.
- (15) Wynne, K. J.; Lambert, J. M. *Silicones*. In *Encyclopedia of Biomaterials and Biomedical Engineering*; Wnek, G. W., Bowlin, G. B., Eds.; Marcel Dekker: New York, 2004; Vol. 1, p 1348.
- (16) Johnston, E.; Bullock, S.; Uilk, J.; Gatenholm, P.; Wynne, K. J. *Macromolecules* **1999**, *32*, 8173.
- (17) Uilk, J.; Bullock, S.; Johnston, E.; Myers, S. A.; Merwin, L.; Wynne, K. J. *Macromolecules* **2000**, *33*, 8791.
- (18) Uilk, J.; Mera, A. E.; Fox, R. B.; Wynne, K. J. *Macromolecules* **2003**, *36*, 3689.
- (19) Bondurant, S.; Ernster, V.; Herdman, R. *Safety of Silicone Breast Implants*; National Academy Press: Washington, D. C., 1999.
- (20) Rajan, G. S.; Sur, G. S.; Mark, J. E.; Schaefer, D. W.; Beaucage, G. J. *Polym. Sci., Part B: Polym. Phys.* **2003**, *41*, 1897.
- (21) LeBaron, P. C.; Pinnavaia, T. J. *Chem. Mater.* **2001**, *13*, 3760.

Scheme 1. Hybrid PDMS Coating Preparation Utilizing Polydiethoxysiloxane (PDES) as the Siliceous Domain (SD) Precursor.



mechanical properties but also to avoid viscosity buildup and nanoparticle aggregation.

In the present research, a modification of “technology” known since 1950²² was used to prepare FSN PDMS hybrids (Scheme 1). In surface analysis by tapping-mode atomic force microscopy (TM-AFM) of the hybrid materials, we found that for certain compositions and cure conditions the near-surface FSN seem to “disappear”.²³ The inability to image near-surface nanoparticles was explained by the formation of an amorphous reticular siliceous surface domain that mechanically isolated near surface nanoparticles. This result showed that nanoparticles can act as “reporters” for secondary siliceous domain structure buildup. Herein, we report surprising new developments for FSN PDMS hybrid nanocomposite materials. Nanoparticles “reappear” or “never appear” depending on composition and nanoparticle surface chemistry. On the basis of information from the reporter nanoparticles, we propose a model for siliceous phase secondary structure buildup that incorporates the TM-AFM results.

PDMS hybrid materials reported herein comprise (1) a low T_g PDMS phase cross-linked by (2) a siliceous domain (SD) generated by in situ hydrolysis/condensation of PDES, and (3) ~ 50 nm fumed silica nanoparticles (FSN; Scheme 1). FSN were either unmodified (U-FSN) or trimethylsilylated (T-FSN). PDES, a low-molecular-weight (<1000) polyalkoxysiloxane is completely miscible with PDMS. If well-mixed (e.g., via a Speed Mixer), the nanocomposites are optically transparent. Details are provided in the Supporting Information.

Condensation-cured PDMS coatings having 14 wt % U-FSN or T-FSN were prepared with 4x, 14x, and 28x ratios of SiOEt to Si-OH. Compositions are designated as before⁵ on the basis of the SiOEt:SiOH ratio, with SiOH from dihydroxyterminated PDMS [$\text{HO}(\text{Me}_2\text{SiO})_n\text{H}$] and SiOEt from PDES. The sample designation T-FSN-14%-14x indicates 14 wt % trimethylsilylated FSN and that the PDES starting mass contained 14 times the molar amount of Si-

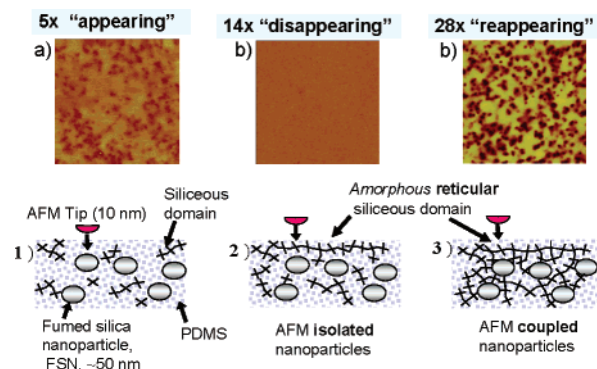


Figure 1. Top: TM-AFM phase images, 500×500 nm, $A/A_0 = 0.60$, for (a) U-FSN-14%-5x; (b) U-FSN-14%-14x; (c) U-FSN-14%-28x. Bottom: Schematic models 1–3 for the respective surface structures of a–c.

OEt groups needed to cross-link $\text{HO}(\text{Me}_2\text{SiO})_n\text{H}$. PDES is used as the crosslinker and siliceous phase precursor as predictable solid-state compositions are obtained.¹⁷ Samples were cured for 3 days at 25°C (90% RH) or 100°C (ambient humidity). From TGA data, the nanocomposites were completely cured after a 3 day cure at 100°C ; water is evolved as evidence of incomplete cure after 3 days at 20°C .²³

Nanocomposites were examined by TM-AFM employing a low setpoint ratio ($A_{sp}/A_0 = 0.6$) generally considered “hard tapping”, as near-surface nanoparticles were usually not imaged at light tapping ($A_{sp}/A_0 \geq 0.9$). For U-FSN-14%-4x (25°C cure), near-surface U-FSN are readily observed in phase-contrast imaging because of the marked difference in modulus between U-FSN versus the PDMS matrix.²³ A typical phase image for U-FSN-14%-4x (25°C) is shown in Figure 1a. An identical phase image is observed after 100°C cure. The results demonstrate that at low volume fractions of siliceous phase, the near-surface nanostructure is independent of cure temperature.²³ Model 1, Figure 1, represents this composition wherein the volume fraction of the siliceous domain is low and fragmented, the AFM tip is unimpeded, and near-surface fumed silica nanoparticles are imaged.

For U-FSN-14%-14x (25°C cure), near-surface U-FSN are also readily observed, but the near-surface image is dramatically changed after 100°C cure (Figure 1b). Even with hard tapping, the near-surface U-FSN “disappear” completely. Model 2 (Figure 1) shows a schematic for the “nanobarrier” formed by the near-surface rigid, amorphous, reticular siliceous domain that precludes observation of near-surface U-FSN. The formation of a siliceous phase nanobarrier for 14x compositions can occur even at room temperature. Condensation cure is slow, so that long cure times and increased catalyst concentration favor more rapid “disappearance” of the fumed silica nanoparticles. The persistent observation of near surface U-FSN is favored by minimizing catalyst concentration (~ 0.3 wt %).

Further to the above, in an investigation of U-FSN-28x compositions, AFM imaging gave completely different results compared to 4x and 14x compositions. Not only are near-surface U-FSN imaged after 25°C cure (Figure 2a), but the image is actually clearer after 100°C cure (Figure 2b). As illustrated in Figure 1, the nanoparticles may be said to “reappear” for U-FSN-28x compositions. Model 3 (Figure

(22) Dow Corning Corp. GB 652754 19510502, 1951.

(23) Ogoshi, T.; Fujiwara, T.; Bertolucci, M.; Galli, G.; Chiellini, E.; Chujo, Y.; Wynne, K. J. *J. Am. Chem. Soc.* **2004**, *126*, 12284.

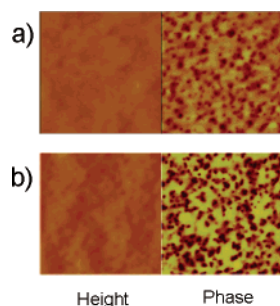


Figure 2. TM-AFM images, 500×500 nm, $A/A_0 = 0.60$, for U-FSN-14%-28x: (a) 25 °C cure; (b) 100 °C cure.

1) is proposed to explain the “reappearance” of U-FSN. For 28x compositions Si–OH groups from the growing siliceous domain react with U-FSN surface Si–OH creating covalent Si–O–Si linkages between the FSN and the SD. In so doing, the larger volume fraction of siliceous phase creates a mechanically rigid connection from the surface to the near-surface nanoparticles. This results a remarkably clear phase image of near-surface U-FSN.

Identical 4x, 14x, and 28x compositions with trimethylsilylated fumed silica nanoparticles (T-FSN) were prepared and investigated by TM-AFM. The results for 4x were similar to that observed for U-FSN compositions shown in Figure 1a. A subtle difference for 14x compositions was observed. Only compositions with minimal catalyst (≤ 0.3 wt %) gave coatings that allowed T-FSN imaging (typically within 24 h) before “disappearance”. Thus, after a 3 day 25 °C cure, T-FSN already “disappeared” and the phase image is similar to Figure 1b. The surprising result compared to U-FSN was that, for 28x compositions containing T-FSN (Figure 3), near-surface nanoparticles are only faintly imaged, regardless of cure conditions.

Model 4 (Figure 3) is proposed to explain the opposite result for near-surface imaging of undetected T-FSN vs clearer imaging of U-FSN in 28x nanocomposites. Model 4 shows trimethylsilylation as a broken circle surrounding T-FSN. The trimethylsilyl groups block access of Si–OH groups on the periphery of the growing siliceous domain. Unlike U-FSN, near-surface trimethylsilylated fumed silica nanoparticles are mechanically isolated from the TM-AFM tip. As a result, near surface T-FSN are not detected by TM-AFM.

By their “disappearance” and “reappearance”, near-surface fumed silica nanoparticles are reporters for buildup of

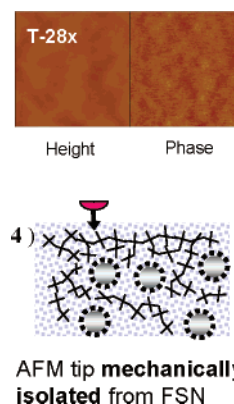


Figure 3. Top: TM-AFM images for T-FSN-14%-28x (25 °C, 3 day cure), 500×500 nm, $A/A_0 = 0.60$. Below: Schematic model 4, see Figure 1 for figure key; exception, broken circle around FSN represents trimethylsilylation.

secondary siliceous domain structure. These results are analogous to what we know on the macroscale (nanoscale model in parentheses): a rock just beneath the water is easily detected by tapping (1). If a thin sheet of ice forms, the rock is no longer detected by tapping (2). If the ice thickens, the rock can once more be detected by tapping because of the mechanical connection of the ice to the rock (3). On the other hand, if the rock is protected by some soft “bumper” layer, we may not easily detect the rock, even when the ice is in direct contact (4). With TM-AFM information from FSN reporters, the model of siliceous phase buildup on the nanoscale directly parallels this macroscale analogy and gives a new insight into the structure of nanocomposites prepared by alkoxysiloxane condensation cure.

Finally, phase images of fracture surface for all compositions and processing conditions are almost identical and always reveal the presence of FSN. Images are similar to those shown in Figure 2; a typical image is provided in the Supporting Information, Figure 1S. The subtle features revealed in the surface study due to buildup of the secondary siliceous phase are destroyed in the fracture process.

Acknowledgment. Research support from U.S. National Science Foundation (DMR-0207560) and the Italian MIUR (PRIN 2005-03-5277) is gratefully acknowledged.

Supporting Information Available: Experimental details and table of nanocomposite compositions. This material is available free of charge via the Internet at <http://pubs.acs.org>.

CM0626839